



King's Research Portal

DOI:

[10.1038/eye.2015.262](https://doi.org/10.1038/eye.2015.262)

Document Version

Peer reviewed version

[Link to publication record in King's Research Portal](#)

Citation for published version (APA):

Steel, D. H. W., Downey, L., Greiner, K., Heimann, H., Jackson, T. L., Koshy, Z., Laidlaw, D. A. H., Wickham, L., & Yang, Y. (2016). The design and validation of an optical coherence tomography-based classification system for focal vitreomacular traction. *Eye (London, England)*, 30(2), 314-324. <https://doi.org/10.1038/eye.2015.262>

Citing this paper

Please note that where the full-text provided on King's Research Portal is the Author Accepted Manuscript or Post-Print version this may differ from the final Published version. If citing, it is advised that you check and use the publisher's definitive version for pagination, volume/issue, and date of publication details. And where the final published version is provided on the Research Portal, if citing you are again advised to check the publisher's website for any subsequent corrections.

General rights

Copyright and moral rights for the publications made accessible in the Research Portal are retained by the authors and/or other copyright owners and it is a condition of accessing publications that users recognize and abide by the legal requirements associated with these rights.

- Users may download and print one copy of any publication from the Research Portal for the purpose of private study or research.
- You may not further distribute the material or use it for any profit-making activity or commercial gain
- You may freely distribute the URL identifying the publication in the Research Portal

Take down policy

If you believe that this document breaches copyright please contact librarypure@kcl.ac.uk providing details, and we will remove access to the work immediately and investigate your claim.

What was known before:

- Isolated vitreomacular traction (VMT) has previously been classified based on the width of vitreous attachment and the presence of macular hole.
- Other associated features of VMT are known to occur but no unified classification system exists to describe them.

What this study adds:

- A simple validated classification system for focal VMT intended to aid in decision-making and prognostication is described.
- It is based on optical coherence tomography and hierarchically classifies seven features of VMT namely **w**idth, **v**itreo-retinal interface changes, **s**hape, **p**igment epithelial changes, **e**levation, and inner and outer **r**etinal changes, under the mnemonic WISPERR.

The design and validation of an optical coherence tomography-based classification system for focal vitreomacular traction

Short title: Classifying focal vitreomacular traction

DHW Steel¹, L Downey², K Greiner³, H Heimann⁴, TL Jackson⁵, Z Koshy⁶, DAH Laidlaw⁷, L Wickham⁸, Y Yang⁹

¹Sunderland Eye Infirmary, Sunderland and Institute of Genetic Medicine, University of Newcastle Upon Tyne, UK

²Ophthalmology Department, Hull and East Yorkshire Eye Hospital, Hull and East Yorkshire NHS Trust, Hull, UK

³Ophthalmology Department, Aberdeen Royal Infirmary, UK

⁴St. Paul's Eye Unit, Royal Liverpool University Hospital, Liverpool, UK

⁵Department of Ophthalmology, School of Medicine, King's College London, London, UK

⁶University Hospital Ayr, Ayr, UK

⁷Ophthalmology Department, St. Thomas' Hospital, London, UK

⁸Ophthalmology Department, Moorfields Eye Hospital, City Road, London, UK

⁹School of Life & Health Sciences, Aston University, Birmingham, UK,

Author for correspondence:

DHW Steel, Sunderland Eye Infirmary, Queen Alexandra Road, Sunderland SR2 9HP, UK

Tel: +44 (0)191 5699065

Fax: +44 (0)191 5699060

E-mail: david.steel@ncl.ac.uk

Word count: 3360

Keywords: vitreomacular traction, vitreomacular adhesion, fovea, optical coherence tomography, ocriplasmin

Disclosures/Conflicts of Interest

This study group was convened by Alcon, which distributes ocriplasmin in the UK on behalf of Thrombogenics. Neither Thrombogenics nor Alcon had input in the design of the study, manuscript preparation, or editorial review and neither were invited to review the manuscript prior to submission. Steel DHW is a consultant to Alcon and advisor to Novartis and Bayer. Jackson TL is a consultant to Thrombogenics and advisor to Alcon, Bausch & Lomb and DORC. Yang Y is a consultant to Bayer and Alimera Sciences and advisor to Alcon, Thrombogenics, Allergan and Novartis. Downey L, Laidlaw DAH, Koshy Z, Heimann H, Wickham L and Greiner K have acted as advisors to Alcon and Thrombogenics regarding ocriplasmin.

Abstract

Purpose:

To develop and validate a classification system for focal vitreomacular traction (VMT) with and without macular hole based on spectral domain optical coherence tomography (SD-OCT), intended to aid in decision-making and prognostication.

Methods:

A panel of retinal specialists convened to develop this system. A literature review followed by discussion on a wide range of cases formed the basis for the proposed classification. Key features on OCT were identified and analysed for their utility in clinical practice. A final classification was devised based on two sequential, independent validation exercises to improve inter-observer variability.

Results:

This classification tool pertains to idiopathic focal VMT assessed by a horizontal line scan using SD-OCT. The system uses width (W), interface features (I), foveal shape (S), retinal pigment epithelial changes (P), elevation of vitreous attachment (E) and inner and outer retinal changes (R) to give the acronym WISPERR. Each category is scored hierarchically. Results from the second independent validation exercise indicated a high level of agreement between graders: intra-class correlation ranged from 0.84 to 0.99 for continuous variables and Fleiss' kappa values ranged from 0.76 to 0.95 for categorical variables.

Conclusions:

We present an OCT-based classification system for focal VMT that allows anatomical detail to be scrutinised and scored qualitatively and quantitatively using a simple, pragmatic algorithm, which may be of value in clinical practice as well as future research studies.

Introduction

Advances in optical coherence tomography (OCT) and, in particular, the recent widespread adoption of spectral domain OCT (SD-OCT), have provided improved visualisation of the vitreoretinal relationships and retinal structure in vitreomacular traction (VMT) syndrome.^{1,2} This has enabled observers to differentiate between the focal variant of VMT sometimes called vitreofoveolar traction (VFT) and the more broadly adherent form of VMT, where the zone of attachment exceeds 1500 microns.^{3,4} The importance of this differentiation is because the latter has a lower probability of undergoing spontaneous separation and, is also less responsive to ocriplasmin.⁵

Although the diagnosis of focal VMT can be easily made on OCT, no study has yet been published detailing those OCT features that might have prognostic significance for either spontaneous remission or progression to a full thickness macular hole. Equally it is not clear which eyes with focal VMT are best suited for intravitreal ocriplasmin. Indeed published series report varying proportions of successful outcome with that treatment modality, as well as with spontaneous resolution or response to vitrectomy.⁶⁻¹⁷

The recently published report by Duker et al¹⁸ has highlighted the OCT features of both the focal and broadly adherent subtypes as well as eyes with focal and broadly adherent interfaces where the retinal architecture is not disrupted, termed vitreo-macular adhesion (VMA). That group also detailed the presence and absence of macular hole in these cases. However the most common presentation of VMT is the focal variant and so there is a need for a more detailed classification of the OCT features that occur in both focal VMA and VMT, with and without a full thickness macular hole.

In this study, we describe the creation and validation of a pragmatic, OCT-based classification system for focal VMT that can be used in clinical practice or future prospective studies to select patients for therapy and evaluate the influence of a wide spectrum of OCT changes on therapeutic outcomes.

Methods

A group of UK consultant retinal specialists was convened with the aim of devising a SD-OCT based classification tool for eyes with focal vitreo-macular adhesions.

A PubMed search for relevant published articles was performed, including only those written in English and published up to November 2013. Selected relevant papers were reviewed prior to the meeting.

Between November 2013 and March 2014 the group met on two occasions. At the first meeting members presented a total of 46 cases of VMT using SD-OCT images from their own practices which helped define the proposed structure of the classification tool. Each feature of the retinal and vitreoretinal interface was systematically explored, before the key elements were identified and reviewed for their utility in assessing VMT in everyday practice.

The group agreed to confine the classification to isolated focal VMA and VMT, and defined those entities as a circumscribed area of vitreofoveal attachment of less than 1500 μm in diameter, with surrounding vitreoretinal separation, and without other retinal disease. VMT, as distinct from VMA, was defined as any associated retinal structural change that was attributed to traction. All retinal change associated with traction, including FTMH, could be included. Conversely VMA was recognized as an adhesion between the hyaloid and macula, but without any structural change in the latter. The minimum scan protocol to be used in grading images, in terms of orientation and position, was defined as a horizontal line scan using SD-OCT through the foveal centre.

The classification system was intended to be practical and user friendly, so data fields should be easy to collate and quantify as well as having validity in clinical practice.

The tool was refined and progressed through a number of iterations via email discussions and at a second meeting, a further 45 case studies were discussed and classified using the prototype tool. A number of exploratory values were added to the classification and a test set of 26 new images of focal VMT were collated and distributed. The 26 images were selected specifically to allow a range of representative features to be evaluated. Images were imported into an open-source image editor (GIMP version 2.8; www.GIMP.org) to

allow linear and angular measurements to be made. The nine clinicians graded the images independently based on the initial classification system. The original classification system used six domains with between two and six categories within each domain, namely:

- 1) The width of vitreous attachment: W
- 2) The nature of the interface between the vitreous and retina: I
- 3) The fovea shape: S
- 4) The presence of retinal pigment epithelium changes: P
- 5) The elevation of the lowest point of vitreous attachment: E
- 6) The nature of associated intra-retinal changes separated into inner and outer retinal changes: R

Categories within each domain were designed to be used in a hierarchical manner. The acronym WISPERR was used as a simple reminder of the various domains. In this version of the classification several additional parameters were also evaluated:

- a) Subdividing the type of inner retinal change into two groups.
- b) Measuring the angle of vitreous insertion into the retinal surface using the method described by Theodossiadis *et al.*¹⁹
- c) Defining the differences between three types of outer retinal change before the occurrence of a FTMH.
- d) Evaluating the ability to discern interface hyper-reflectivity in the zone of VMT.

The test results were analysed for inter-observer agreement using intra-class correlation (ICC) for continuous variables and two-way analysis of variance to assess for any systematic bias between observers. In addition, we used the method of Jones *et al.*²⁰ to assess agreement between observers and to produce an estimate of the limits of agreement with the mean. Fleiss' kappa was used for categorical variables. Fleiss' kappa is a measure of the closeness of agreement between multiple raters employing a categorical scale. The data are considered categorical rather than ordinal, so no credit is given for close agreement as in a weighted kappa: the latter can only be applied to paired observations. The values of ICC and Fleiss' kappa can be interpreted as follows: 0–0.2 indicates poor agreement; 0.3–0.4 indicates fair agreement; 0.5–0.6 indicates moderate agreement; 0.7–0.8 indicates strong

agreement; and >0.8 indicates almost perfect agreement. We were thus able to provide an overall measure of reliability and agreement between the ratings used and evaluate the reproducibility of the scale in each category of the proposed classification

Disagreements were identified and definitions reviewed. Categories with high levels of disagreement where separate entities could not be consistently discerned were either merged or removed. In particular, the angular measurements and the subdivision of the inner retinal changes were removed because of low agreement, and the shape and interface classifications were simplified. The definitions of the outer retinal changes were also revised to provide greater clarity. Based on these results and discussions a final classification was produced and named WISPERR (Table 1, with illustrative figures defining the features used shown in Figure 1). A further test set of 10 new cases was reviewed and agreement between group members was assessed again.

Results from both test sets are presented.

A series of examples of the classification using real images is shown in Figure S1 (supplementary information online).

Results

Initial test set of 26 images

The width of vitreous attachment in the image set ranged from a case of narrow VMT, which the observers measured at a mean of 22 μm , to a case of broad VMT measured at a mean of 1040 μm . The ICC between observers was 0.98 ($F=0.84$, $P=0.67$). The measurements showed no systematic relationship with width or image and the limit of agreement with the mean was 32.3 μm , which we considered clinically acceptable.

The elevation of the lowest point of vitreoretinal adhesion ranged from a mean of 275 μm to a mean of 760 μm . The ICC between observers was 0.84 ($F=1.07$, $P=0.38$). The measurements showed no systematic relationship with degree of elevation or image and the limit of agreement with the mean was 29.6 μm , which was clinically acceptable.

For the purposes of the test evaluation the base diameter of outer retinal dehiscence and FTMHs were measured. For outer retinal dehiscence (n=7), the base diameter ranged from 128 μm to 820 μm ; the ICC between observers was 0.99 ($F=1.22$, $P=0.31$). For FTMHs (n=5), the minimum linear diameter ranged from 160 μm to 346 μm ; the ICC between observers was 0.84 ($F=1.84$, $P=0.15$). The measurements showed no systematic relationship with width or image and the limit of agreement with the mean was 15.3 μm for base diameter and 26.2 μm for the minimum linear diameter.

The angle of insertion of the vitreous into the retina measured from 12 to 67 degrees on the nasal side of the VMT and from 11 to 69 degrees temporally. There was limited variation between the mean of observers for all measurements and variation between readers was consistent but the ICC showed only moderate agreement (0.69) and ANOVA suggested strong evidence of systematic bias between observers ($F=5.21$, $P<0.00001$). The limits of agreement showed no obvious relationship with angle size but some angles showed tighter measurements than others, with the maximum variation in any one angle varying by up to 27 degrees between observers. The limit of agreement with the mean measured 9.6 degrees. We considered this to be clinically significant and hence excluded angle assessments, as they were too unreliable to be included in the classification.

Fleiss' kappa values varied between 0.61 for the vitreoretinal interface and 0.78 for the presence of retinal pigment epithelium (RPE) abnormality (Table 2a).

Final test set of 10 images using final grading scheme

In this test set only the categorical sections were re-evaluated (Table 2b), with improved Fleiss' kappa values of 0.76–0.95.

Discussion

The proposed classification system focuses on focal VMT (isolated VFT) rather than all types of VMT. The International Vitreomacular Traction Study Group recently published a

classification system of vitreoretinal interface abnormalities, including VMT.¹⁸ Although comprehensive, it is not sufficiently detailed regarding focal VMT to allow the discovery of new prognostic indicators. Other classifications have also been proposed^{4,8,21} but none to date have included the wide range of features that clinicians use to assess focal VMT.

In a stepwise iterative process, we initially selected vitreoretinal features that were either previously known to be important, or those that the group considered may influence VMT progression, resolution or response to treatment. Importantly, these characteristics had to be easily assessable, with a clear definition to allow acceptable reproducibility in a real-world (rather than a grading centre) setting. This stepwise system allowed consensus to be reached and improved the classification's validity. The high agreement values in the final classification reflect this. We purposefully designed the classification to be hierarchical for ease of use. It should be noted that although only OCT features are included in the classification, non-OCT features remain important.

The classification is designed to be used with SD-OCT and principally a single horizontal line scan through the foveal centre. Other scans, however, should be utilised to further define the extent of the VMA, aid in the detection of eccentric areas of macular hole and ERM, and to delineate the maximum values of the minimum linear diameters of FTMHs. It is important that the scan through the middle of the foveola is selected. This is defined as the area with no bipolar or ganglion cells and where the dark band of the outer nuclear layer extends to the foveal surface, without an intervening outer plexiform layer (Figure 2). Clinicians should be wary of using eccentric OCT slices as these will confound the assessment. It should also be noted when interpreting scans that at the foveal centre on SD-OCT, the area between the ellipsoid zone and the retinal pigment epithelium (RPE) can appear slightly lucent and wider than adjacent areas. Furthermore, the inner retinal surfaces are brighter on the horizontal surfaces, especially nasally where the nerve fibre layer is thickest (Figure 2).

The width of the VMA is the primary feature for differentiation between classically recognised VMT and VFT.^{4,21} Width has been demonstrated as predictive of treatment outcome with intravitreal ocriplasmin⁹ and shown to be prognostic of spontaneous release.^{22,23} This feature of VMA exists as a continuum rather than a discrete value^{4,16} and we therefore determined that it should be measured. The longest continuous length of

adhesion is likely to be the most important in terms of release rather than the sum of discontinuous areas of focal VMT, and therefore this was chosen for the classification. Although the surface area of the adhesion has been evaluated as a prognostic measure of VMT separation²³ measuring this in a clinic setting would necessitate a specified scan protocol, which varies between machines and centres.

Concerning the vitreoretinal interface itself, as ERM is known to be a feature of VMT and related to both the chance of spontaneous separation and separation induced by ocriplasmin, this was included. We separated retinal surface ERM from changes specifically at the area of VMT itself and further divided ERM that was contiguous with the zone of VMT from non-contiguous ERM. Interface opacity at the zone of VMT, both hyper-reflectivity and increased thickness, was found to be a variable feature on the scans examined by the group and could be reliably detected. It has previously been shown to be prognostic of release with plasmin.^{24,25} We did not observe any cases of VMT associated with the recently described entity of lamellar hole associated epiretinal proliferation.²⁶

Although the shape of the fovea is currently not known to be a prognostic factor, it is important in distinguishing VMT from VMA and correlates with the width of adhesion and elevation to suggest the extent of traction. In this study, we sub classified shape into normal, loss of inner retinal profile or eversion of fovea. This simple categorisation of shape had good agreement between the graders. Eversion of the fovea may prove useful in future investigation of visual function in VMT, as found in recent studies on diabetic macular oedema.^{27,28}

The classification was not designed to be used with for VMA in conjunction with other diseases, such as wet age-related macular degeneration, diabetic maculopathy or retinal vein occlusion. However, we frequently noted that some cases of otherwise isolated VMT had concomitant features of ageing, including RPE atrophy and small drusen. Additionally, in chronic VMT there can be changes in the uniformity of the RPE pigment with pigment migration,^{29,30} so a simple categorisation of the presence or absence of RPE changes has been included.

Elevation is an objective measure of the severity of VMT. Many OCT machines provide an automated measure of maximum foveal height but with tenuous focal VMT we found that segmentation errors were common using automated protocols. We therefore included a manual measurement of the height from the RPE to the lowest point of VMA to allow for cases with partially avulsed inner retinal flaps.

It is well established that there is a positive relationship between the tension exerted by differing widths of VMT and alterations in retinal architecture.^{16,19,31} Observation of cases has shown that inner retinal changes are more common, and that outer retinal changes can range from subtle alterations at the level of the outer segments of the photoreceptors to outer retinal dehiscence and FTMHs.³² Recently, however, Almeida *et al*²² noted that eyes with isolated inner retinal distortion but without outer retinal changes have an apparently higher incidence of spontaneous vitreomacular separation than those with outer retinal changes. We therefore separated inner retinal change recording from outer retinal change.

A variety of inner retinal changes have been described and named in tractional maculopathies. Some authors have also attempted to differentiate between inner retinal changes that may be associated with VMT (variously described as foveal cavitation, foveolar cysts, foveal cystoid spaces)³³ versus cystoid macular oedema^{33,29} and retinoschisis.² We found, however, that the observers could not reproducibly differentiate these entities, so a single division of present or not present was included. A measure of the degree of inner retinal change is also coded within the classification by the elevation measurement.

Similarly, a large number of outer retinal changes have been described, including a localised opalescence of the ellipsoid zone termed the 'cotton ball' sign, thought to be due to traction at the foveola, which disappears upon vitreoretinal release.^{25,34} Other changes reported include localised defects of the ellipsoid zone and/or exterior limiting membrane, which can be associated with the presence of ERM.³⁵⁻³⁸ These are all included in one category as distinguishing between them was inconsistent between observers. We differentiated subretinal fluid from more subtle outer retinal changes and also from outer retinal dehiscence seen in impending macular holes. The latter occurs as a result of tractional forces on the outer retina.^{39,40} It has been shown that following treatment of VMT, while

intraretinal cystic changes resolve quickly, subretinal fluid resolves more slowly during longer follow up.⁴¹

When considering the assessment of FTMH, measurement of the maximum of the minimum linear diameter is included, as this measurement has been used in the majority of publications to date. It is defined as the width of the narrowest hole diameter using a line drawn parallel to the RPE. The narrowest part of the hole should be measured, other than that involving the associated retinal operculum—the exact location of the narrowest part of the hole varies with the hole configuration (Figure 3). To find the maximum measurement, the OCT slice with the widest macular hole width should be used—this can be facilitated by using a dense horizontal line scanning protocol or using multiple radial scans. Base diameter of macular holes is however, a more reproducible measurement⁴² and was included to quantify the extent of outer retinal dehiscence in cases without FTMH. It is important that in cases of outer retinal dehiscence the presence of an eccentric full thickness defect is not missed by utilising a dense scanning protocol as with FTMH (Figure 3).

We initially included the angle of vitreous insertion into the VMT relative to the RPE. Theodossiadis *et al*¹⁷ described an increasing angle of vitreous insertion as being predictive of VMT spontaneous resolution. However, this was subsequently removed from the classification due to the high variability of measurements between observers. Furthermore, although angles may be useful in a research setting their measurement is confounded by a number of variables including scan orientation and the aspect ratio the scan is viewed at. Furthermore OCT scans are typically presented with the retina viewed as a planar surface rather than the reality, which is a concave curved surface,⁴³ which will also alter the VMT angles measured.

In conclusion, we present a novel classification system for focal VMT with details of its design and validation. We hope it will serve as a pragmatic system that clinicians could use in routine clinical practice and in collaborative research studies to investigate new prognostic features related to functional and anatomical outcomes, either with treatment or observation.

Acknowledgements

Dr Wickham acknowledges financial support from the Department of Health through the award made by the National Institute for Health Research to Moorfields Eye Hospital NHS Foundation Trust and UCL Institute of Ophthalmology for a Specialist Biomedical Research Centre for Ophthalmology.

Conflict of Interest

This study group was convened by Alcon, which distributes ocriplasmin in the UK on behalf of Thrombogenics. Neither Thrombogenics nor Alcon had input in the design of the study, manuscript preparation, or editorial review and neither were invited to review the manuscript prior to submission. Steel DHW is a consultant to Alcon and advisor to Novartis and Bayer. Jackson TL is a consultant to Thrombogenics and advisor to Alcon, Bausch & Lomb and DORC. Yang Y is a consultant to Bayer and Alimera Sciences and advisor to Alcon, Thrombogenics, Allergan and Novartis. Downey L, Laidlaw DAH, Koshy Z, Heimann H, Wickham L and Greiner K have acted as advisors to Alcon and Thrombogenics regarding ocriplasmin.

Supplementary information is available at Eye's website.

References

1. Do DV, Cho M, Nguyen QD, Shah SM, Handa JT, Campochiaro PA *et al.* Impact of optical coherence tomography on surgical decision making for epiretinal membranes and vitreomacular traction. *Retina* 2007; **27**: 552–556.
2. Folgar FA, Toth CA, DeCroos FC, Girach A, Pakola S, Jaffe GJ. Assessment of retinal morphology with spectral and time domain OCT in the phase III trials of enzymatic vitreolysis. *Invest Ophthalmol Vis Sci* 2012; **53**: 7395–7401.
3. Johnson MW. Perifoveal vitreous detachment and its macular complications. *Trans Am Ophthalmol Soc* 2005; **103**: 537–567.
4. Bottós J, Elizalde J, Rodrigues EB, Farah M, Maia M. Classifications of vitreomacular traction syndrome: diameter vs morphology. *Eye* 2014; **28**: 1107–1112.
5. Singh RP, Li A, Bedi R, Srivastava S, Sears JE, Ehlers JP *et al.* Anatomical and visual outcomes following ocriplasmin treatment for symptomatic vitreomacular traction syndrome. *Br J Ophthalmol* 2014; **98**: 356–360.
6. Hickichi T, Yoshida A, Trempe CL. Course of vitreomacular traction syndrome. *Am J Ophthalmol* 1995; **119**: 55–61.
7. Codenotti M, Maestranzi G, De Benedetto U, Querques G, Della Valle P, Iuliano L *et al.* Vitreomacular traction syndrome: a comparison of treatment with intravitreal plasmin enzyme vs spontaneous vitreous separation without treatment. *Eye* 2013; **27**: 22–27.
8. John VJ, Flynn HW Jr, Smiddy WE, Carver A, Leonard R, Tabandeh H, Boyer DS. Clinical course of vitreomacular adhesion managed by initial observation. *Retina* 2014; **34**: 442–446.

9. Stalmans P, Benz MS, Gandorfer A, Kampik A, Girach A, Pakola S *et al*. Enzymatic vitreolysis with ocriplasmin for vitreomacular traction and macular holes. *N Engl J Med* 2012; **367**: 606–615.
10. Kim BT, Schwartz SG, Smiddy WE, Doshi RR, Kovach JL, Berrocal AM *et al*. Initial outcomes following intravitreal ocriplasmin for treatment of symptomatic vitreomacular adhesion. *Ophthalmic Surg Lasers Imaging Retina* 2013; **44**: 334–343.
11. Haller JA, Stalmans P, Benz MS, Gandorfer A, Pakola SJ, Girach A *et al*. Efficacy of intravitreal ocriplasmin for treatment of vitreomacular adhesion: subgroup analyses from two randomized trials. *Ophthalmology* 2015; **122**: 117–122.
12. Yamada N, Kishi S. Tomographic features and surgical outcomes of vitreomacular traction syndrome. *Am J Ophthalmol* 2005; **139**: 112–117.
13. Mazit C, Scholtes F, Rabaut C, Jallet G, Cochereau I. Assessment of macular profile using optical coherence tomography after epiretinal membrane surgery. *J Fr Ophtalmol* 2008; **31**: 667–672.
14. Sayegh RG, Georgopoulos M, Geitzenauer W, Simader C, Kiss C, Schmidt-Erfurth U. High-resolution optical coherence tomography after surgery for vitreomacular traction: a 2-year follow-up. *Ophthalmology* 2010; **117**: 2010–2017.
15. Sonmez K, Capone A Jr, Trese MT, Williams GA. Vitreomacular traction syndrome: impact of anatomical configuration on anatomical and visual outcomes. *Retina* 2008; **28**: 1207–1214.

16. Bottós J, Elizalde J, Arevalo JF, Rodrigues EB, Maia M. Vitreomacular traction syndrome. *J Ophthalmic Vis Res* 2012; **7**: 148–161.
17. Theodossiadis GP, Grigoropoulos VG, Theodoropoulou S, Datseris I, Theodossiadis PG. Spontaneous resolution of vitreomacular traction demonstrated by spectral-domain optical coherence tomography. *Am J Ophthalmol* 2014; **157**: 842–851.
18. Duker JS, Kaiser PK, Binder S, de Smet MD, Gaudric A, Reichel E *et al*. The International Vitreomacular Traction Study Group classification of vitreomacular adhesion, traction, and macular hole. *Ophthalmology* 2013; **120**: 2611–2619.
19. Theodossiadis G, Petrou P, Eleftheriadou M, Moustakas AL, Datseris I, Theodossiadis P. Focal vitreomacular traction: a prospective study of the evolution to macular hole: the mathematical approach. *Eye* 2014; **28**: 1452–1460.
20. Jones M, Dobson A, O'Brian S. A graphical method for assessing agreement with the mean between multiple observers using continuous measures. *Int J Epidemiol* 2011; **40**: 1308–1313.
21. Johnson MW. Posterior vitreous detachment: evolution and complications of its early stages. *Am J Ophthalmol* 2010; **149**: 371–382.
22. Almeida DR, Chin EK, Rahim K, Folk JC, Russell SR. Factors associated with spontaneous release of vitreomacular traction. *Retina* 2015; **35**: 492–497.
23. Codenotti M, Iuliano L, Fogliato G, Querques G, Bandello F. A novel spectral-domain optical coherence tomography model to estimate changes in vitreomacular traction syndrome. *Graefes Arch Clin Exp Ophthalmol* 2014; **252**: 1729–1735.

24. Elbendary AM, Elwan MM, Azzam HA, Eldeeb DR. Predictability of vitreous detachment following intravitreal plasmin injection in diabetic macular edema associated with vitreomacular traction. *Curr Eye Res* 2011; **36**: 534–539.
25. Tsunoda K, Watanabe K, Akiyama K, Usui T, Noda T. Highly reflective foveal region in optical coherence tomography in eyes with vitreomacular traction or epiretinal membrane. *Ophthalmology* 2012; **119**: 581–587..
26. Pang CE, Spaide RF, Freund KB. Epiretinal proliferation seen in association with lamellar macular holes: a distinct clinical entity. *Retina* 2014; **34**: 1513–1523.
27. Giovannini A, Amato G, Mariotti C, Scassellati-Sforzolini B. Optical coherence tomography findings in diabetic macular edema before and after vitrectomy. *Ophthalmic Surg Lasers* 2000; **31**: 187–191.
28. Kiire CA, Broadgate S, Halford S, Chong V. Diabetic macular edema with foveal eversion shows a distinct cytokine profile to other forms of diabetic macular edema in patients with type 2 diabetes. *Invest Ophthalmol Vis Sci* 2014; **55**(13): 4408 (abstract C0264).
29. Chang LK, Fine HF, Spaide RF, Koizumi H, Grossniklaus HE. Ultrastructural correlation of spectral-domain optical coherence tomographic findings in vitreomacular traction syndrome. *Am J Ophthalmol* 2008; **146**: 121–127.
30. Georgopoulos M, Geitzenauer W, Ahlers C, Simader C, Scholda C, Schmidt-Erfurth U. High-resolution optical coherence tomography to evaluate vitreomacular traction before and after membrane peeling. *Ophthalmologe* 2008; **105**: 753–760.

31. Spaide RF, Wong D, Fisher Y, Goldbaum M. Correlation of vitreous attachment and foveal deformation in early macular hole states. *Am J Ophthalmol* 2002; **133**: 226–229.
32. Takahashi A, Yoshida A, Nagaoka T, Takamiya A, Sato E, Kagokawa H *et al*. Idiopathic full-thickness macular holes and the vitreomacular interface: a high-resolution spectral-domain optical coherence tomography study. *Am J Ophthalmol* 2012; **154**: 881–892.
33. Koizumi H, Spaide RF, Fisher YL, Freund KB, Klancnik JM Mr, Yannuzzi LA. Three-dimensional evaluation of vitreomacular traction and epiretinal membrane using spectral-domain optical coherence tomography. *Am J Ophthalmol* 2008; **145**: 509–517.
34. Uemura A, Otsuji F, Nakano T, Sakamoto T. Vitreomacular interface and outer foveal microstructure in fellow eyes of patients with unilateral macular holes. *Retina* 2014; **34**: 1229–1234.
35. Itoh Y, Inoue M, Rii T, Hirota K, Hirakata A. Correlation between foveal cone outer segment tips line and visual recovery after epiretinal membrane surgery. *Invest Ophthalmol Vis Sci* 2013; **54**: 7302–7308.
36. Okamoto F, Sugiura Y, Okamoto Y, Hiraoka T, Oshika T. Associations between metamorphopsia and foveal microstructure in patients with epiretinal membrane. *Invest Ophthalmol Vis Sci* 2012; **53**: 6770–6775.
37. Bottoni F, De Angelis S, Luccarelli S, Cigada M, Staurenghi G. The dynamic healing process of idiopathic macular holes after surgical repair: a spectral-domain optical coherence tomography study. *Invest Ophthalmol Vis Sci* 2011; **52**: 4439–4446.

38. Ooka E, Mitamura Y, Baba T, Kitahashi M, Oshitari T, Yamamoto S. Foveal microstructure on spectral-domain optical coherence tomographic images and visual function after macular hole surgery. *Am J Ophthalmol* 2011; **152**: 283–290.
39. Gaudric A, Haouchine B, Massin P, Paques M, Blain P, Erginay A. Macular hole formation: new data provided by optical coherence tomography. *Arch Ophthalmol* 1999; **117**: 744–751.
40. Haouchine B, Massin P, Gaudric A. Foveal pseudocyst as the first step in macular hole formation: a prospective study by optical coherence tomography. *Ophthalmology* 2001; **108**: 15–22.
41. Uchino E, Uemura A, Doi N, Ohba N. Postsurgical evaluation of idiopathic macular traction syndrome by optical coherence tomography. *Am J Ophthalmol* 2001; **132**: 122–123.
42. Wakely L, Rahman R, Stephenson J. A comparison of several methods of macular hole measurement using optical coherence tomography, and their value in predicting anatomical and visual outcomes. *Br J Ophthalmol* 2012; **96**: 1003–1007.
43. Kuo AN, McNabb RP, Chiu SJ, El-Dairi MA, Farsiu S, Toth CA, Izatt JA. Correction of ocular shape in retinal optical coherence tomography and effect on current clinical measures. *Am J Ophthalmol* 2013; **156**: 304–311.

Titles and legends to figures

Table 1 The focal VMT classification tool: WISPERR.

Table 2 Fleiss' kappa values

Figure 1 Schematic representation of the focal VMT classification tool: WISPERR. (a) Width of vitreous attachment (W), interface features (I) and foveal shape (S). (b) Retinal pigment epithelial changes (P), elevation of vitreous attachment (E) and inner and outer retinal changes (R).

Figure 2 Horizontal SD-OCT of a normal fovea. *Note pre-macula bursa.

Figure 3 Examples of minimum linear diameter measurements using SD-OCT slice with maximum hole dimensions. In A the minimum linear diameter is on the inner side of the hole and in an eccentric slice without vitreomacular traction, whilst in B it is on the outer retinal side of the hole. C shows a case of apparent outer retinal dehiscence but with a tiny para-central full thickness macular hole seen on one more eccentric OCT slice in D. When measuring minimum linear diameter, the area of the retinal operculum should not be included (shown in E and F).

[Supplementary information]

A series of examples of the WISPERR classification system using real OCT images.

Supplementary Figure S1a Examples of focal vitreomacular traction with or without full thickness macular hole classified using the WISPERR system.

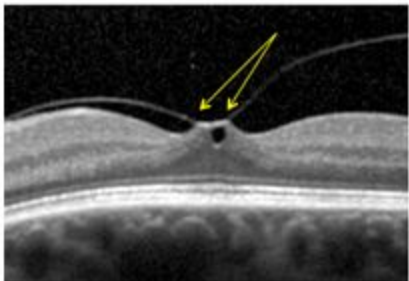
Supplementary Figure S1b Examples of focal vitreomacular traction with or without full thickness macular hole classified using the WISPERR system.

Supplementary Figure S1c Examples of focal vitreomacular traction with or without full thickness macular hole classified using the WISPERR system.

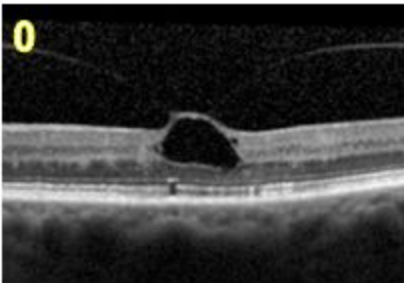
Figure 1a. The focal vitreomacular traction classification tool: WISPERR

Width

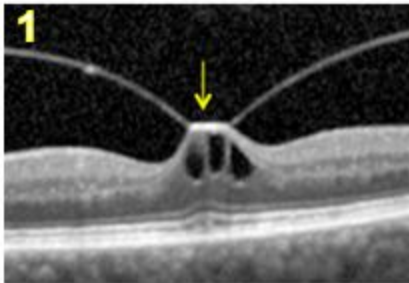
Width of longest measurable VR adhesion extent on any scan which is connected to the foveal centre – if there are multiple areas the longest single one should be used.



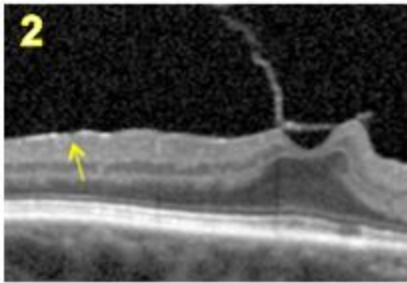
Interface



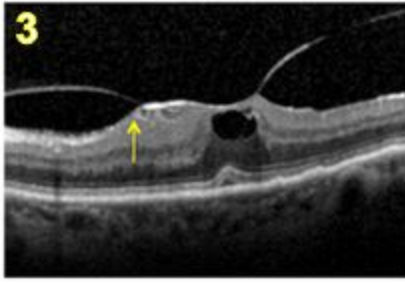
None



Hyper-reflective inner retinal signal on area of VMA

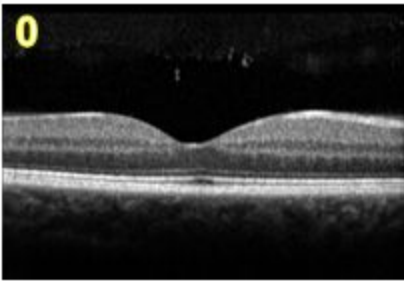


ERM on any part of the area of retina encompassed by the OCT

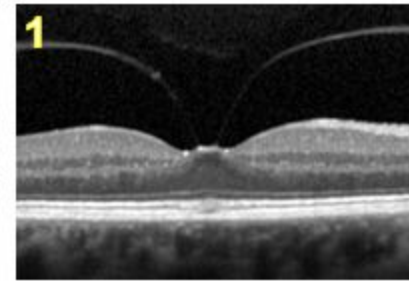


ERM within the central 1mm ETDRS circle or contiguous with VMT.

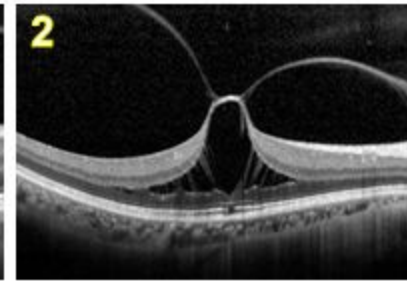
Shape



Normal



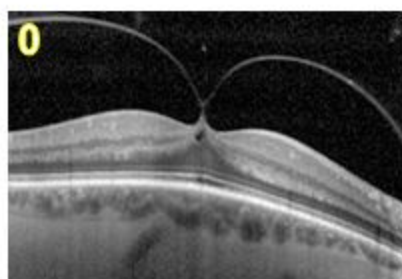
Abnormal profile with loss of smooth contour e.g. notch or flat profile.



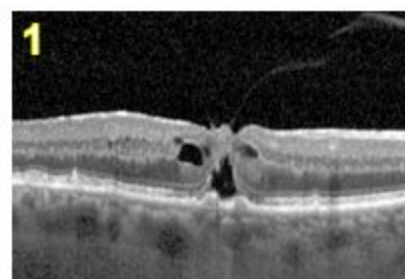
Clear eversion of the central foveola with convex profile of the central fovea.

Figure 1b. The vitreomacular traction classification tool: WISPERR

**Pigment
Epithelium
disturbance**

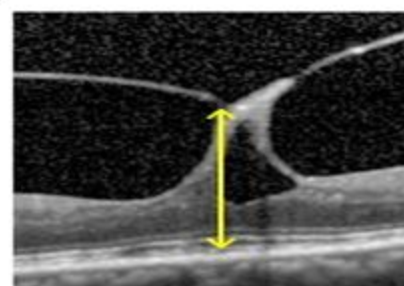
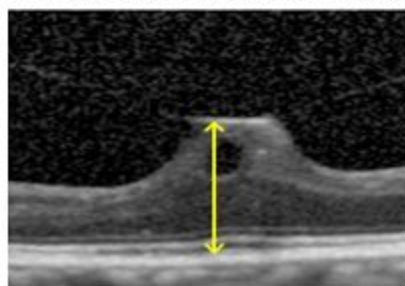
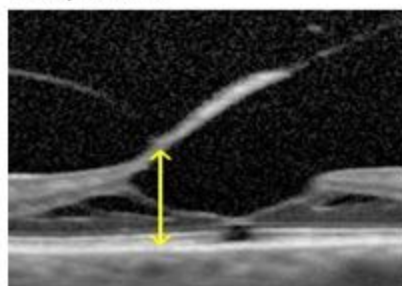


Not present



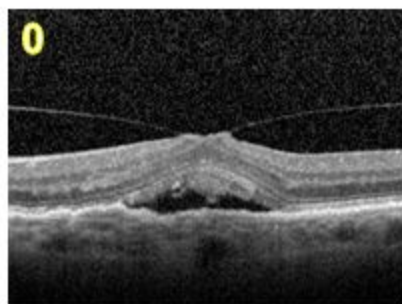
Present e.g. drusen, RPE atrophy

Elevation

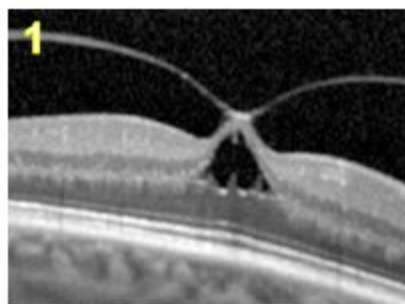


Maximum retinal thickness in central 1 mm diameter ETDRS circle – measured from inner surface of RPE to the point of lowest vitreoretinal adhesion and including any SRF.

**Retina
Inner Retina**

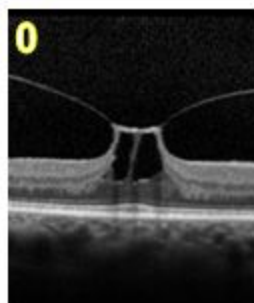


Normal

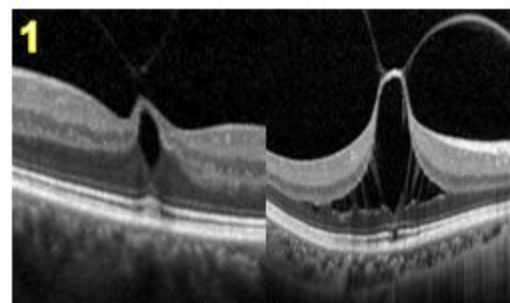


Inner retinal cysts or cleavage

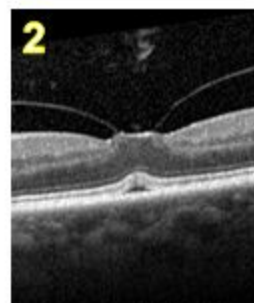
**Retina
Outer Retina**



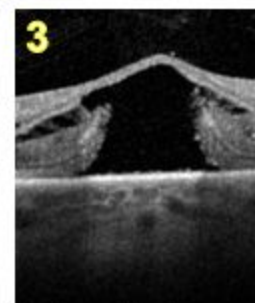
None



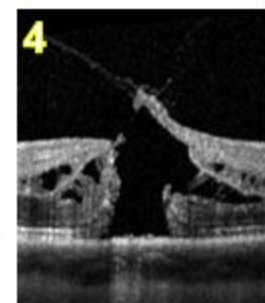
Focal outer retinal abnormality without SRF, or dehiscence



Sub-retinal fluid



Outer retinal dehiscence



FTMH

Figure 2

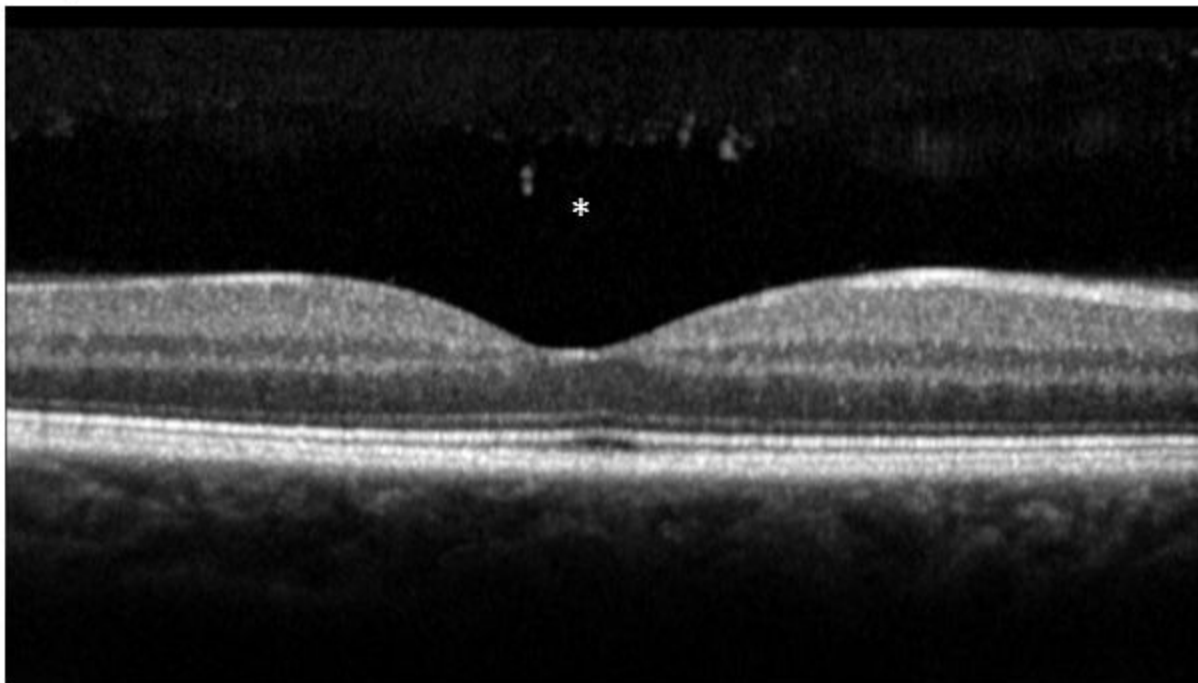


Figure 3

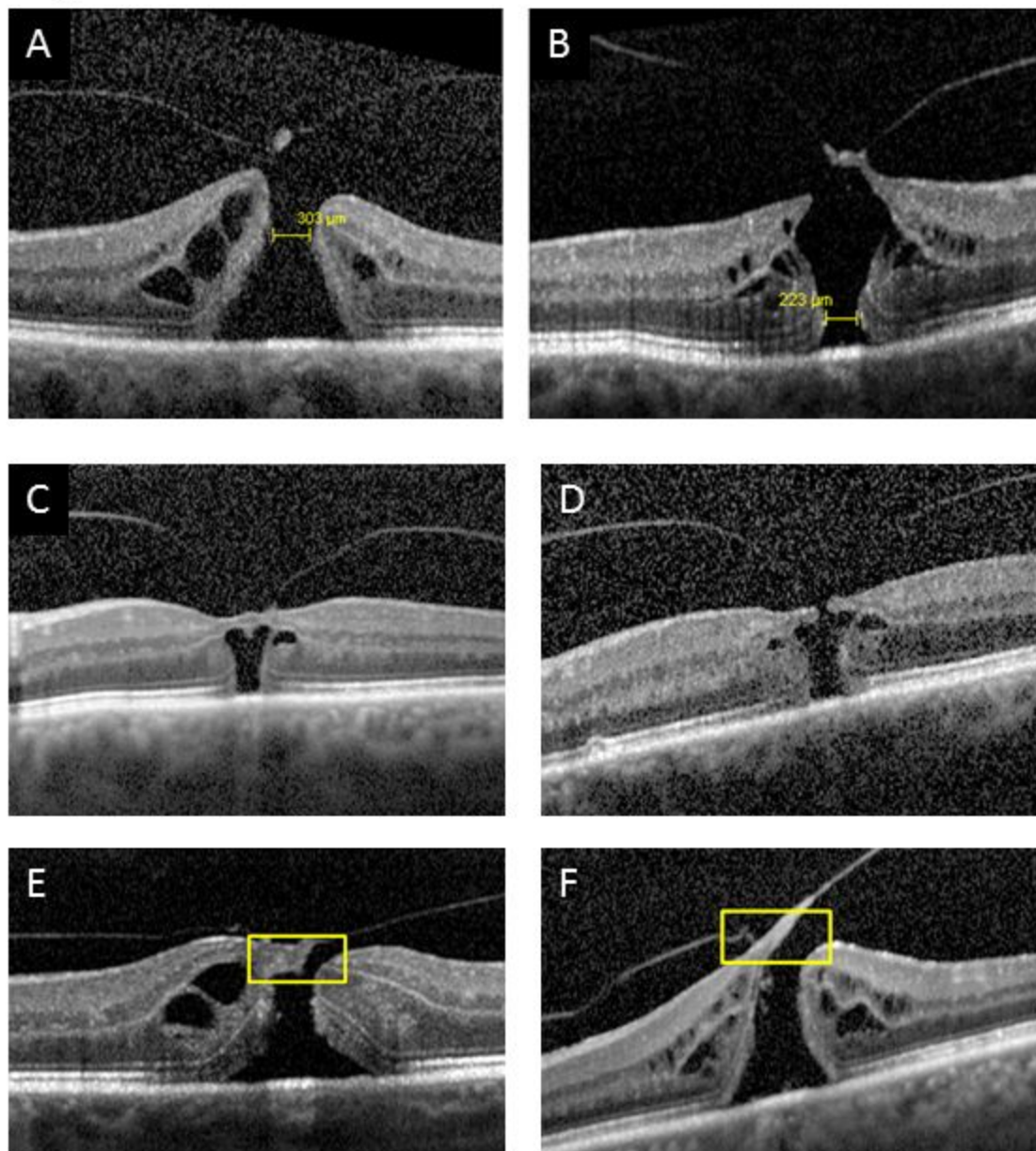


Table 1 The focal VMT classification tool: WISPERR.

Letter	Feature classified	Description of measurement technique or feature	Units of measurement or graded categories
W	Width of vitreo-macular attachment	Width of longest measurable vitreo-macular adhesion extent on any scan which is connected to the foveal centre—if there are multiple areas of adhesion the longest single one should be used.	Measurement in microns.
I	Interface between retina and vitreous cavity	Surface membrane.	<p>0) None.</p> <p>1) Hyper-reflective inner retinal signal on the VMA itself compared to adjacent retina (indicative of thickened ILM and can include thickened ILM alone and/or pre ILM material which has not met criteria for an ERM).</p> <p>2) Any ERM on any part of the area of retina encompassed by the OCT (signified by a discrete line anterior to ILM surface, retinal corrugations and discrete areas of high signal on ILM).</p> <p>3) Any ERM within the central 1-mm ETDRS circle or contiguous with the zone of VMT.</p>
S	Shape	Foveal shape based on foveal profile and position as compared to surrounding retina.	<p>0) Normal.</p> <p>1) Abnormal profile with loss of smooth contour e.g. notch formation, concave with loss of depression relative to other side, asymmetry of depression or flat profile.</p> <p>2) Clear eversion of the central foveola with a convex profile of the central fovea.</p>
P	Pigment epithelium	Presence of RPE abnormalities in central ETDRS 1-mm diameter circle.	<p>0) Not present.</p> <p>1) Present (could include drusen and/or RPE atrophy).</p>

E	Elevation of retinal surface from RPE	Height of maximum central retinal thickness in central 1-mm diameter ETDRS circle—measured from inner surface of RPE to maximum retinal elevation and therefore including any SRF.*	Measurement in microns.*
R1	Inner retina	Inner retinal changes within central 3-mm ETDRS circle.	0) Normal. 1) Inner retinal cysts or cleavage.
R2	Outer Retina	Outer retinal changes within central 3-mm ETDRS circle.	0) None. 1) Focal outer retinal abnormality (including ‘cotton ball’ sign, IS/OS/ELM disruption/fragmentation) without SRF, or dehiscence . 2) SRF with outer retinal separation of the photoreceptors from the RPE with upward displacement of IS/OS and ELM lines (including with hypo- or hyper-reflective filling of the resultant space). Usually associated with irregularity of photoreceptor outer segments but no actual defects or dehiscence 3) Outer retinal dehiscence , i.e. sharply-defined defect in the outer retina involving at least the ellipsoid zone and ELM secondary to photoreceptor separation with a layer of intact inner retina. Size of defect measured as base diameter.** 4) Full thickness macular hole and ‘maximum minimum’ horizontal linear dimension.***

*Many OCT systems measure this in an automated way but it is best measured manually to avoid segmentation errors. In cases where there is a partially avulsed flap of retina or an oblique highest point, the height to the lowest point of contiguous vitreoretinal adhesion should be used.

**The maximum base diameter should be measured horizontally from the two junctions of the outer retina with RPE. A dense scanning protocol should be followed to avoid missing small eccentric full thickness macular holes.

***The maximum of the minimum linear diameter is measured—this is defined as the narrowest hole diameter in the mid-retina using a line drawn parallel to the RPE. The narrowest part of hole should be measured other than that involving the hole operculum. To find the maximum measurement the OCT slice with the widest macular hole width should be used—this can be facilitated by using a dense horizontal line-scanning protocol or using multiple radial scans.

Abbreviations: ELM, exterior limiting membrane; ERM, epiretinal membrane; ETDRS, Early Treatment Diabetic Retinopathy Study, ILM, inner limiting membrane; IS, inner segment; OCT, optical coherence tomography; OS, outer segment; RPE, retinal pigment epithelium; SRF, subretinal fluid; VMA, vitreomacular adhesion; VMT, vitreomacular traction.

Table 2 Fleiss' kappa values

a. Initial test set of 26 images.

	Fleiss' kappa	95% confidence interval
Vitreoretinal interface	0.61	0.55–0.67
Shape	0.71	0.65–0.76
Presence of RPE abnormality	0.78	0.71–0.85
Inner retina	0.63	0.55–0.71
Outer retina	0.71	0.66–0.76

b. Final test set of 10 images.

	Fleiss' kappa	95% confidence interval
Vitreoretinal interface	0.81	0.75–0.86
Shape	0.82	0.74–0.88
Presence of RPE abnormality	0.76	0.71–0.81
Inner retina	0.95	0.91–0.99
Outer retina	0.79	0.73–0.85

Abbreviations: RPE, retinal pigment epithelium.